Monitoring of the ANTARES optical module efficiencies using ^{40}K decays in sea water

I. Salvadori[*] **and V. Kulikovskiy**

Aix Marseille Univ, CNRS/IN2P3, CPPM, Marseille, France
E-mail: salvadori@cppm.in2p3.fr, kulikovskiy@cppm.in2p3.fr

On behalf of the ANTARES Collaboration

Using the data collected by the ANTARES neutrino telescope from 2009 to 2016, the optical module (OM) efficiencies have been determined through the so called ^{40}K method. The results have been computed on a 6-day basis, after applying selection cuts in order to provide reliable time-dependent OM efficiencies for most of the individual OMs. The results show an impressive stability over time, as well as the benefit of the high voltage tuning (HVT), which is a dedicated procedure aimed to keep efficiencies at their best.

---

[*]Speaker.

1. Introduction

^{40}K is the most abundant radioactive isotope in sea water. Its Cherenkov light spectrum is equal to the one produced by muons detected by the ANTARES neutrino telescope [1]. It constitutes the principal source of background light. However, ^{40}K is as well an important calibration tool. In ANTARES, the optical modules (OMs) are arranged in groups of three (storey) and, if a ^{40}K decays near a storey, its Cherenkov light can be recorded by two OMs simultaneously. Such coincidences are dominated by ^{40}K, therefore the measured rates can be used to tune the overall OM efficiency in a detailed GEANT4 [5] simulation of the OM. This simulation provides valuable input for the global detector simulation.

The document is organized as follows: in Section 2 a brief description of the ANTARES neutrino telescope is given; the ^{40}K method for the computation of the OM efficiencies is described in Section 3; in Section 4 the used data set is presented; the fitting procedure together with the quality cuts applied are explained in Section 5, while the results of the analysis are presented in Section 6. In Section 7 a brief description of GEANT4 dedicated simulations for the overall OM efficiency is given. Conclusions and an outlook to the next generation of neutrino telescopes in the Mediterranean Sea are given in Section 8.

2. The ANTARES neutrino telescope

The ANTARES neutrino telescope was deployed in the Mediterranean Sea, 40 km from the coast of Toulon (France), at a depth of around 2.4 km. It was completed in 2008. The main goal of ANTARES is, at high energies, the study of energetic astrophysical objects. However, at lower energies, neutrino oscillations can be measured by analyzing distortions in the energy/angular spectrum of upward-going atmospheric neutrinos.
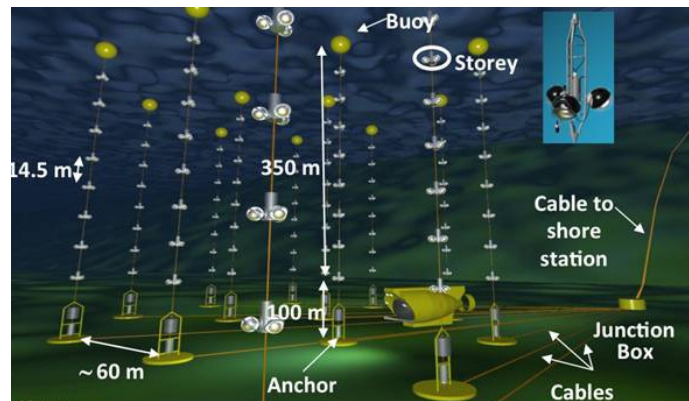

Figure 1: Schematic representation of the ANTARES neutrino telescope [2].

ANTARES is composed of 12 detection lines, each one equipped with 25 floors of 3 optical modules. Each OM holds a photomultiplier tube (PMT). The horizontal spacing among the lines is around 60 m, while the vertical spacing between the storeys is around 15 m (see Figure 1). The OMs in a storey are arranged in such a way that the axis of the PMTs points 45° downwards (see Figure 2). The photomultipliers are 10-inch tubes from Hamamatsu. The relative positions of all

OMs in the detector are monitored in real time by a dedicated positioning system.

When the distribution of the fitted charge of all PMTs in the detector shows either a broadening or a shift with respect to its nominal value, resulting in losses of efficiency and trigger bias, a dedicated procedure of high voltage tuning (HVT) is performed. The aim of this operation is to reset the effective threshold to its canonical value.
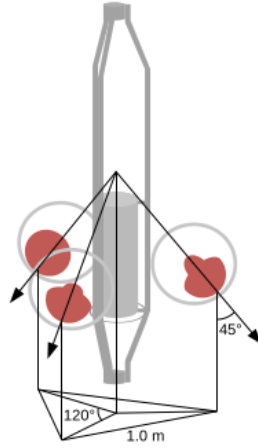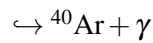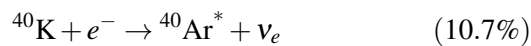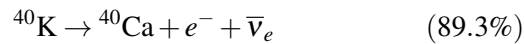

Figure 2: Schematic representation of an ANTARES storey [3]. The spheres stand for the OMs, which contain one PMT each, facing $45°$ downwards.

3. The ^{40}K Method

The main decay channels of ^{40}K are β decay and electron capture:

$$^{40}\text{K} \rightarrow {}^{40}\text{Ca} + e^- + \overline{\nu}_e \qquad (89.3\%)$$

$$^{40}\text{K} + e^- \rightarrow {}^{40}\text{Ar}^* + \nu_e \qquad (10.7\%)$$

$$\hookrightarrow {}^{40}\text{Ar} + \gamma$$

The free electron produced in the first decay channel induces Cherenkov light emission when traveling in water; fast electrons with subsequent Cherenkov light emission are also produced by Compton scattering of the photon produced by the excited Argon nuclei.

In ANTARES, if a ^{40}K decays near a storey, its Cherenkov light can be recorded by two OMs simultaneously: this is called a *genuine* coincidence. There exists also a background of *random* coincidences, which happens when two hits by two different ^{40}K decays appear to be close in time. By plotting these signals as a function of the time differences between the two OMs, the shape is that of a flat uniform background due to the random coincidences plus a Gaussian peak from the genuine coincidences. An example of such distribution is shown in Figure 3.
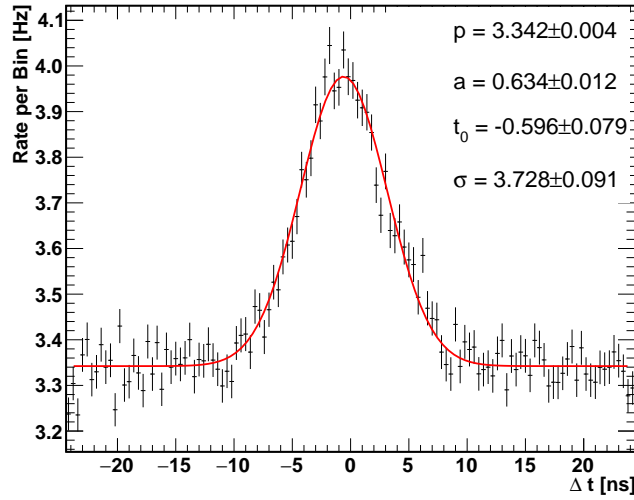
Figure 3: Example of the detected hit time differences, from ^{40}K background, between two optical modules.

The histogram of the coincidence signal is fitted with a Gaussian distribution plus a uniform one:

$$f(t) = p + a \cdot \exp(-\frac{(t-t_0)^2}{2\sigma^2}) \tag{3.1}$$

where p is the baseline, a the amplitude of the Gaussian peak due to genuine coincidences, σ is the peak width and t_0 the time offset. A mean value of $\sigma \sim 4$ ns is expected, due to the spatial distribution of the ^{40}K decays around the storey. The maximal travel distance for two photons emitted at the same place and detected by two different OMs of the same floor is the sum of the OMs distance (~ 1 m) and the photocatode diameter (~ 25 cm); considering the Cherenkov light velocity of 0.22 m/ns a time difference of 5.6 ns is expected. By averaging over the whole space a result compatible with 4 ns is found.

For perfectly calibrated OMs, t_0 would be expected at 0 ns. Deviations from the expected value of t_0 are mainly due to imperfections in time calibration. This makes the ^{40}K method also a useful tool to cross check the time calibration. However in the following we concentrate on the derivation of relative OM efficiencies from ^{40}K data.

The fit parameters can then be used to estimate the rate of events corresponding to the peak area, as:

$$R = \frac{a \cdot \sigma \cdot \sqrt{2\pi}}{T \cdot \Delta\tau} \tag{3.2}$$

where $\Delta\tau$ is the bin length used for the histogram (in this work $\Delta\tau = 0.4$ ns), and T is the total lifetime of the data set.

For each detector storey three coincidence rates are measured (R_{01}, R_{12} and R_{20}). These quantities are directly related to the sensitivities of the three OMs (s_0, s_1 and s_2):

$$R_{ij} = R^* s_i s_j \qquad (3.3)$$

where R^* is the rate for two nominal OMs with sensitivities equal to 1. In this work a value of $R^* = 15$ Hz was used. It was obtained as an average detector coincidence rate at the beginning of the analyzed data set. Solving the system of three equations the corresponding sensitivities are derived:

$$s_0 = \sqrt{\frac{1}{R^*}\frac{R_{01}R_{20}}{R_{12}}}, s_1 = \sqrt{\frac{1}{R^*}\frac{R_{12}R_{01}}{R_{20}}}, s_2 = \sqrt{\frac{1}{R^*}\frac{R_{20}R_{12}}{R_{01}}} \qquad (3.4)$$

When an OM is broken, only one coincidence histogram is filled, which is not enough to determine the two efficiencies. In this case, equal sensitivities for the two working OMs are assumed, namely:

$$s_i = s_j = \sqrt{\frac{R_{ij}}{R^*}} \qquad (3.5)$$

4. Data Set

Data collected from October 2009 to December 2016 have been used in this work. A dedicated ^{40}K trigger was used during the data-taking. For this trigger, coincidence hits in adjacent OMs are stored if they occur within a narrow time window of typically 50 ns. The trigger is applied with an important down-scaling factor of 200 in order not to saturate the readout chain. Taking into account this scaling factor, a total lifetime of 11 days has been analyzed. The runs have been collected in groups of 6 calendar days, which corresponds to a lifetime of around 40 minutes for each data point.

5. Procedure

The coincidence histograms are filled whenever the Δt between hits is within a maximally allowed time window, which for this work has been set to 90 ns, larger than the typical trigger time window.

All the coincidence histograms have then been fitted accordingly to Equation 3.1, from -24 ns to $+24$ ns, and some quality cuts have been applied, to ensure stable and reliable input for the subsequent efficiency calculation. The first cut on the number of entries of the histogram excludes from the analysis all those cases for which the fit fails due to lack of statistics. Taking into account the number of fitted parameters and the binning of the coincidence histograms, a χ^2 of around 116 is expected, thus, histograms with $\chi^2 > 200$ are excluded. Additional cuts on the amplitude value and its uncertainty have been applied to ensure a clear signal above background. Furthermore, expected values of the Gaussian mean and width are known, thus cuts on these parameters have been applied, in order to avoid cases in which the fit falls outside the allowed regions.

6. Results

The histograms which passed the quality cuts are then used to compute the OM efficiency, as described in Section 3. For each period analyzed, an average over all the non-zero efficiency OMs is performed. Figure 4 shows the global detector information on the OM efficiencies as a function of time.
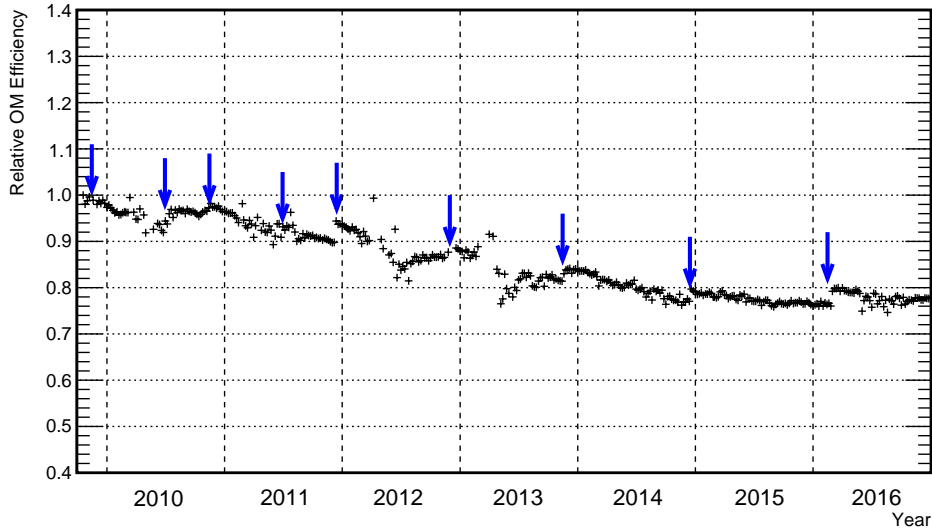

Figure 4: Relative OM efficiency over all the detector as a function of time. The blue arrows indicate the periods in which the HVT has been performed.

The values are normalized according to the first analyzed period. It can be seen that, despite the expected drop in efficiency, due to the ageing of the OMs and the consequences of biofouling, the ANTARES OMs show an impressive stability over time. An average decrease of the OM efficiency by 20%, as observed from 2009 to 2016, leads to a drop of selected atmospheric neutrino events of around 35%. However, a hypothetical astrophysical signal with a E^{-2} flux would decrease only of 15%. The effects of the HVT procedure, which is usually performed once or twice per year and allows to recover the overall efficiency periodically, can be observed as well.

7. Detailed OM calibration with simulations and ^{40}K rates

A detailed simulation is used in ANTARES to estimate the OM effective area and its dependence on the photon incident angle and wavelength [4]. These estimations are the key ingredients for the full detector simulation.

The light detection in OMs is modeled using the latest GEANT4 library [5]. A precise simulation of the photon interaction in the photocathode is performed, taking into account the optical properties of bialkali photocathodes and using a dedicated algorithm [6]. The simulation accurately reproduces the geometry of the OMs, including the glass sphere and the gel, which holds the PMT in place.

The simulation is done till the photoelectron escapes to the PMT vacuum and further signal

detection is calculated via collection efficiency, which is parameterized as a function of the photo-electron production point on the photocathode. The shape of this function is obtained by comparing PMT scans with lasers, and simulations. The absolute value of the function is tuned in order to reproduce a ^{40}K coincidence rate of 15 Hz. This is reached by setting the collection efficiency to $\sim 80\%$ at the PMT center which is physically well motivated.

8. Conclusions and Outlook

Using data collected by the ANTARES neutrino telescope with a dedicated ^{40}K trigger, the OM efficiencies have been computed until the end of 2016. The results show a good stability over time. The ^{40}K method can also be used to cross check the time calibration. The individual time dependent OM efficiencies, as calculated with the procedure presented here, are used on all recent ANTARES physics analyses.

The next generation of neutrino telescopes in the Mediterranean Sea is called KM3NeT [7]. It will be constituted by two main detectors, ARCA (Astroparticle Research with Cosmics in the Abyss), in Sicily, devoted to high energy studies, and ORCA (Oscillation Research with Cosmics in the Abyss), in France, optimised for GeV atmospheric neutrinos. The general detector layouts are similar to the one of ANTARES, with a series of detection lines, each one equipped with floors of digital optical modules (DOMs). The main difference is that each floor hosts 31 PMTs, instead of three. This allows to collect not only double coincidences from ^{40}K decays, but also multiple ones, improving the technique to compute the DOMs efficiencies as well as to study and discriminate background light.

References

[1] ANTARES Collaboration, *ANTARES: the first undersea neutrino telescope*, *Nucl.Instrum.Meth.* A656 11-38 (2011).

[2] http://antares.in2p3.fr.

[3] ANTARES Collaboration, *Measurement of the atmospheric muon flux with a 4 GeV threshold in the ANTARES neutrino telescope*, *Astropart.Phys.*, **33**, 86-90 (2010).

[4] C. M. F. Hugon, *GEANT4 simulation of optical modules in neutrino telescopes*, *PoS(ICRC2015)1106*.

[5] http://geant4.web.cern.ch/geant4/.

[6] D. Motta and S. Schönert, *Optical properties of bialkali photocathodes*, *NIM A , 539 (2005) 217 - 235*.

[7] KM3NeT Collaboration, *Letter of Intent for KM3NeT 2.0*, *Journal of Physics G: Nuclear and Particle Physics*, **43** (8) 084001 (2016).